Modelling of silicon oxynitridation by nitrous oxide using the reaction rate approach

Christophe Krzeminski

Journal of Applied Physics

Modelling of silicon oxynitridation by nitrous oxide using the reaction rate approach

Cite as: J. Appl. Phys. **114**, 224501 (2013); https://doi.org/10.1063/1.4839675
Submitted: 17 July 2013 • Accepted: 15 November 2013 • Published Online: 09 December 2013

Christophe Dominique Krzeminski

Modelling of silicon oxynitridation by nitrous oxide using the reaction rate approach

Christophe Dominique Krzeminski[a)]
Départment ISEN, IEMN-UMR-8520, 41 Boulevard Vauban, 59046 Lille Cedex, France

(Received 17 July 2013; accepted 15 November 2013; published online 9 December 2013)

Large technological progress in oxynitridation processing leads to the introduction of silicon oxynitride as ultra-thin gate oxide. On the theoretical side, few studies have been dedicated to the process modelling of oxynitridation. Such an objective is a considerable challenge regarding the various atomistic mechanisms occurring during this fabrication step. In this article, some progress performed to adapt the reaction rate approach for the modelling of oxynitride growth by a nitrous ambient are reported. The Ellis and Buhrman's approach is used for the gas phase decomposition modelling. Taking into account the mass balance of the species at the interface between the oxynitride and silicon, a minimal kinetic model describing the oxide growth has been calibrated and implemented. The influence of nitrogen on the reaction rate has been introduced in an empirical way. The oxidation kinetics predicted with this minimal model compares well with several experiments. © *2013 AIP Publishing LLC*. [http://dx.doi.org/10.1063/1.4839675]

I. INTRODUCTION

Silicon oxynitridation is a routinely fabrication process used by the semiconductor industry to replace the classical silicon dioxide in the gate processing of logic transistor devices even for the most advanced technological node.[1,2] The main interest of oxynitridation is related to the nitrogen incorporation at the interface which improves (i) the silicon interface passivation (with the reduction of electrically active defects or traps),[3] (ii) the breakdown properties,[4] and (iii) the reliability.[5] Several methods reported the fabrication of silicon oxynitride (SiO_xN_y). Most of them are based on different ambients such as: (i) ammonium (NH_3) nitridation,[6,7] (ii) nitric oxide (NO),[8–11] and (iii) oxidation by nitrous oxide (N_2O).[12–15] Despite the relatively low concentration of nitrogen incorporated, the oxides grown in a nitrous oxide ambient are known to generate a gate oxide with an excellent quality and reliability.[16]

A better understanding of the O_2 and nitrogen distribution during the different processes is necessary for gate stack optimization. To date, for classical dry or wet silicon oxidation, the phenomenological model of Deal and Grove remains used to describe the oxide growth kinetics in a process simulator.[17] Assuming a steady state for the reaction between the oxidizing agent and silicon, Deal and Grove deduced that the oxide growth can simply be described by this analytical linear-parabolic relationship as a function of the oxidation time. In the specific case of N_2O oxynitridation, only preliminary studies are available in the literature.[18–20] For example, some models propose a modified version of the Deal and Grove[18] or Massoud's model[19] to take into account the influence of nitrogen on oxidation kinetics. A fully parametric approach was also suggested in order to fit the kinetics by an empirical time dependent law.[20] However, nobody has been proposed a physical model able to describe the nitrogen incorporation and its profile engineering.[21–24] The main purpose of this paper is to present some progress towards this objective with the build-up of an extended oxynitridation model and the calibration of a minimal one able to describe the oxide growth.

II. GAS PHASE DECOMPOSITION MODELLING

Initially, N_2O is the unique constituent of the oxidizing gas phase. The various species concentration generated during the decomposition of the N_2O molecule is needed. Several approaches were published[25–27] in order to simulate the gas phase decomposition of the N_2O molecule. These three models are based on the chemistry of NO_x compounds which are intensively studied in another research domain (air pollution and combustion reactions). The main differences between these different models are the description level and the number of reactions considered to describe the decomposition. Up to eighty different chemical reactions can be formulated for the most complex one.[25] The approach of Ellis and Buhrman[27] has been preferred since the N_2O gas phase decomposition can be simulated with a simple eight reaction scheme.

A. Reaction scheme

The next system of Eqs. (1) described the following reaction scheme:

$$\begin{cases} N_2O + M \xrightarrow{(k_1)} N_2 + O^* + M & (R_1) \\ N_2O + O^* \xrightarrow{(k_2)} 2NO & (R_2) \\ N_2O + O^* \xrightarrow{(k_3)} N_2 + O_2 & (R_3) \\ O^* + O^* + M \xrightarrow{(k_4)} O_2 + M & (R_4) \\ O^* + NO + M \xrightarrow{(k_5)} NO_2 + M & (R_5) \\ O^* + NO_2 \xrightarrow{(k_6)} NO + O_2 & (R_6) \\ O^* + O^* + wall \xrightarrow{(k_7)} O_2 & (R_7) \\ 2NO_2 \xrightarrow{(k_8)} 2NO + O_2 & (R_8), \end{cases} \quad (1)$$

[a)]christophe.krzeminski@isen.fr

where

$$M = N_2O + N_2 + O_2 + NO + NO_2 + O^* . \quad (2)$$

Factor *M* corresponds to the different collision partners and is equal to the sum of the different species in the furnace. During the decomposition process, five different compounds are generated: molecular nitrogen (N_2), molecular oxygen (O_2), nitric oxide (NO), nitrogen dioxide (NO_2), and atomic oxygen (O*). At the beginning of the reaction (R_1), the N_2O molecule activates the decomposition. This reaction is the most important one since it initiates the N_2 decomposition: the main products created by the first reaction (R_1) are N_2 and O*. O* is the most important one in the reaction scheme since this radical is involved in six reactions out of eight. The two reactions (R_2 and R_3) increase the decomposition and lead to the creation of new products (NO, O_2, and N_2O). At the end of the reaction, only three main compounds remain: N_2, O_2, and NO. Each reaction ($x : 1 \rightarrow 8$) is activated by a rate described by an Arrhenius law

$$k_x = k_{0x} \exp\left(\frac{-E_x}{k_b T}\right), \quad (3)$$

where x corresponds to the reaction R_x. E_x is the activation energy and k_{0x} is the pre-exponential factor. The various concentrations are given in mol/cm^3. As shown in Figure 1, the reaction rate of reaction R_1 is defined by three different Arrhenius laws. Each temperature range is described in Table I. However, the other reaction rates from (k_2 to k_8) follow more classical expressions as shown in Table II.

The evolution for each species is described by the reaction rate approach which postulates that for a general second order reaction

$$a[A] + b[B] \xrightarrow{k(T)} c[C] + d[D] , \quad (4)$$

the decay rate of the [*A*] specie is given by

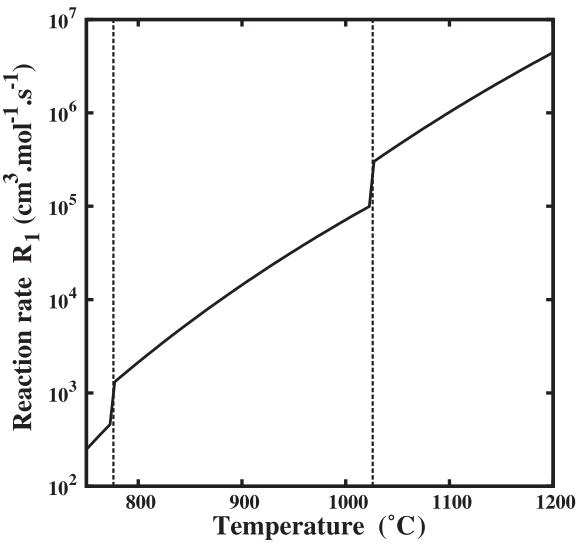

FIG. 1. Variation of the reaction rate coefficient R_1 using the parameters from Table I.

TABLE I. Arrhenius parameters for reaction (R_1) governing the N_2O decomposition. The units for the pre-exponential factor are $cm^3 \cdot mol^{-1} \cdot s^{-1}$. Activation energies are given in eV.

T(K)	k_{01}	E_1 (eV)
[1300–2500]	$5 \times 10^{+14}$	2.5
[1050–1300]	$1.1 \times 10^{+13}$	2.07
[900–1050]	$2.7 \times 10^{+15}$	2.57

$$\frac{d[A]}{dt} = -ak(T)[A]^a[B]^b. \quad (5)$$

Applying this framework with the previous reaction scheme described by Eq. (1), (R_1) → (R_8) leads to a system of six coupled differential equations able to simulate the evolution of the different species

$$\frac{\partial[N_2O]}{\partial t} = -k_1[N_2O][M] - (k_2 + k_3)[N_2O][O^*], \quad (6)$$

$$\frac{\partial[NO]}{\partial t} = 2k_2[N_2O][O^*] - k_5[O][NO][M] + k_6[NO_2][O^*] + 2k_8[NO_2][NO_2], \quad (7)$$

$$\frac{\partial[N_2]}{\partial t} = k_1[N_2O][M] + k_3[N_2O][O^*], \quad (8)$$

$$\frac{\partial[O^*]}{\partial t} = k_1[N_2O][M] - (k_2 + k_3)[N_2O][O^*] - (k_4[M] + k_7)[O^*]^2 - k_5[O^*][NO][M] - k_6[O^*][NO_2], \quad (9)$$

$$\frac{\partial[O_2]}{\partial t} = k_3[N_2O][O^*] + (k_4[M] + k_7)[O]^2 + k_3[O][N_2O] - k_5[O][NO][M] + k_6[O^*][NO_2] + k_8[NO_2]^2, \quad (10)$$

$$\frac{\partial[NO_2]}{\partial t} = k_5[O^*][NO][M] - k_6[O^*][NO_2] - 2k_8[NO_2]^2. \quad (11)$$

A five order Runge-Kutta algorithm using an adaptive step was used in order to solve the equations system.[28] The main

TABLE II. Arrhenius parameters for the other reactions (R_2) → (R_8). The units for the pre-exponential factor are $cm^3 \cdot mol^{-1} \cdot s^{-1}$ for second order reactions (R_2, R_3, R_6, R_8) and $cm^6 \cdot mol^{-2} \cdot s^{-1}$ for third order reactions (R_4, R_5).

Reaction	k_{0x}	$E_x(eV)$
(R_2)	$1.0 \times 10^{+13}$	0.078
(R_3)	$1.0 \times 10^{+14}$	1.210
(R_4)	$1.0 \times 10^{+14}$	1.210
(R_5)	$1.0 \times 10^{+15}$	−0.081
(R_6)	$1.0 \times 10^{+13}$	0.026
(R_7)	$0.0 \times 10^{+13}$	0.026
(R_8)	$2.0 \times 10^{+12}$	1.160

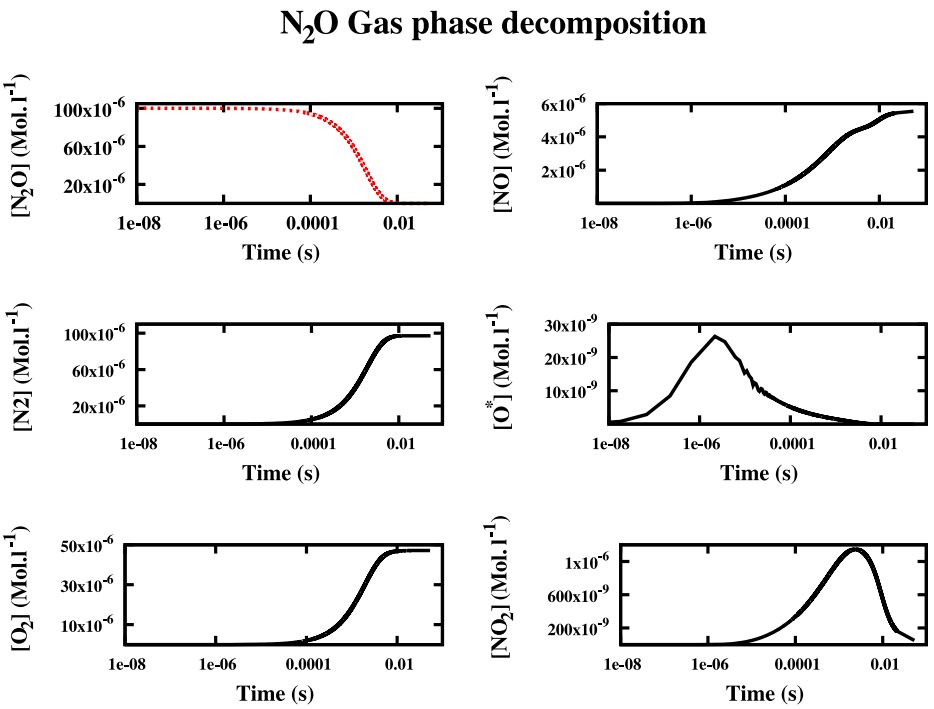

FIG. 2. Evolution of the different species during gas phase decomposition at 1200 °C.

concern with the numerical resolution of this system is that the reaction rate of R_5 is very high and thus, a very short initial time-step is necessary ($\sim$1 ps). An initial ambient made of pure N_2O at a concentration of 1×10^{-04} mol/cm^3 was also considered.

B. Results

The N_2O half-life time as function of the furnace temperature is reported in Figure 2. It corresponds to the time necessary to reach 50% of decay in the initial gas phase concentration. It is clear that the decomposition is very fast at a high temperature (less than 0.1 ms at 1200 °C) but increases linearly with decreasing temperature. For example, at 750 °C, the half-time life is closed to 20 s. A large time indicating that the decomposition could not be complete at the end of the temperature ramp-up during furnace oxynitridation. The half-time life value of the N_2O molecule extracted is directly comparable to those of Tobin *et al.*[29] obtained by a simple two-reaction scheme. The three discontinuities of the half-life time are directly linked to the variation assumed for reaction rate k_1 for the reaction R_1.

Next, the evolution at 1200 °C of the different species (N_2O, N_2, O_2, O*, NO, NO_2) during decomposition is reported in Figure 2. The N_2O concentration decay is very effective between [10^{-4}-10^{-2}]s which is in agreement with the value of the half-life time (0.1 ms at 1200 °C) previously calculated. The first compounds formed around 10^{-7}s are O* and N_2 through reaction R_1. As shown in Figure 3, the O* concentration increases slowly and reaches a maximum at 10^{-5} s. At this time, reactions R_3 and R_2 do not contribute to the N_2O decomposition since O* is in sufficient concentration to create mostly N_2, O_2, and NO compounds. It can be observed that reaction R_2 is the main source of nitric oxide NO. During this step, a small amount of NO_2 is created. The NO_2 concentration reaches its maximum at 5×10^{-3} s. The decomposition of this molecule increases the amount of NO concentration generated through reactions R_6 and R_8. These results stress the key role of O* in the generation of NO.

Finally, the gas phase steady state composition as a function of the furnace temperature is given in Figure 4 since the remaining products play a major role in the oxynitridation process. A key result is that the final ambient contains only three different species: N_2, O_2, and NO and is not so far from a dry oxidation diluted with nitrogen (N). The amount of NO generated is generally very small (less than 3% of the ambient). A zoom provided by Figure 5 on the NO concentration increase shows that a high temperature is beneficial.

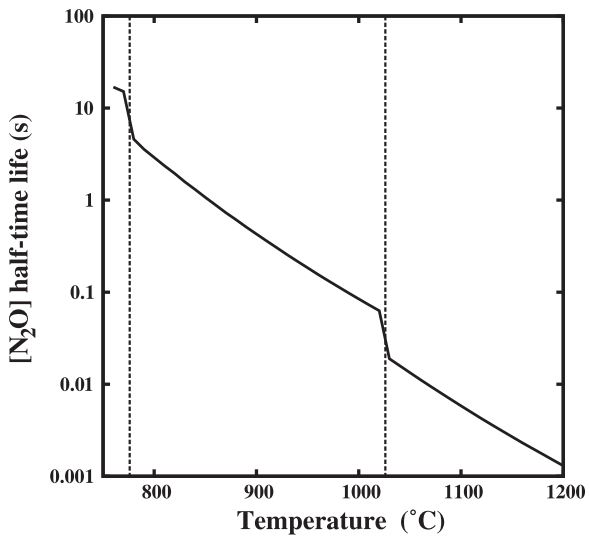

FIG. 3. The evolution of the steady state concentration of the three species resulting from the decomposition (N_2O, O_2, NO) in function of the furnace temperature.

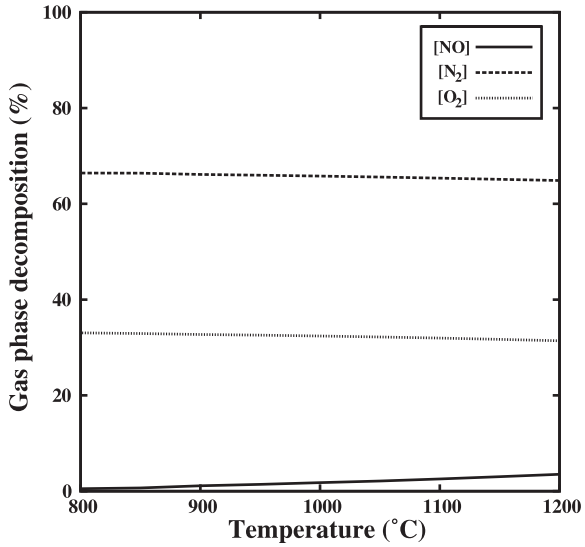

FIG. 4. The half-time life of the N_2O molecule is simulated as a function of the furnace temperature. The decomposition of N_2O is less effective at low temperatures (less than 0.1 ms at 1200 °C).

III. A COMPACT MODEL FOR N_2O OXYNITRIDATION

Several publications highlight that the reaction rate approach is of particular interest in order to provide a more physical alternative to the Deal and Grove model for ultra-thin oxidation.[30–32] The basic idea governing this approach is to estimate the different species during the reaction with the Si substrate in order to overcome the main assumption of the Deal and Grove model (i.e., stationarity and a sharp interface). In this framework, the development of a compact model able to simulate the N_2O oxynitridation step is presented. First, the system considered is specified. Next, the main reactions with the Si substrate during oxynitridation and their mathematical formulation are reported.

A. System description

A schematic of the system considered is reported in Figure 6. The Si substrate can be viewed as a Si monolayers

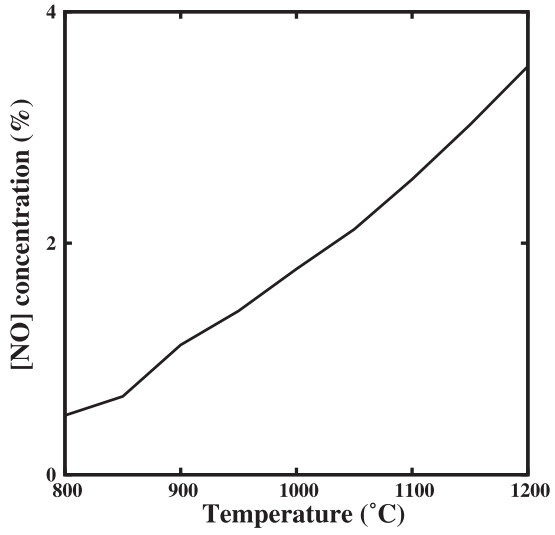

FIG. 5. Focus on the evolution of the NO concentration in function of the furnace temperature.

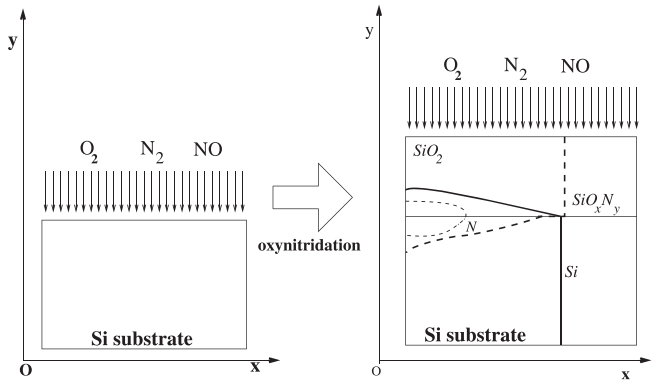

FIG. 6. Schematic view of the system model. The profile of Si, SiO_2, and nitrogen concentration are presented and lead to the definition of two different layers: the oxynitride SiO_xN_y and the Si part.

assembly in interaction with the gas phase. In order to simulate an ultra-thin oxidation, a one dimensional mesh matching the oxidation of the [100] silicon surface is assumed. This means that the vertical resolution of the mesh corresponds to the distance between two Si planes (1.35 Å). The first node is associated to the gas phase. The film growth is restricted to the vertical direction. Thanks to the previous results concerning the gas phase decomposition, it can be reasonably assumed that the decomposition of the N_2O gas is complete and that the ambient is composed of O_2, N_2, and NO.[33] In the substrate, two silicon based species Si and SiO_2 are considered. A new specie SiN (Ref. 34) was introduced to take the formation between N and Si into account. In order to describe the evolution of the species j (where $j = O_2$, NO, Si, SiO_2, SiN), their normalized concentration n_j can be defined by

$$n_j(x,y,t) = \frac{C_j(x,y,t)}{C_j^0}, \tag{12}$$

where C_j corresponds to the planar concentration in units of the number of atoms per surface unit and C_j^0 is the maximum possible concentration in the plane. n_j corresponds to the layer coverage. For example, a value of 1 for n_{Si} means that the layer coverage is complete and corresponds to a concentration of 0.91×10^{15} at/cm^2 of silicon.

B. Main reactions with the silicon substrate

Based on the previous result of the gas phase decomposition, the N_2O oxynitridation process is approximated as shown in Figure 7 as mostly a dry oxidation process with in parallel, an oxynitridation step made by nitric oxide. In a previous work,[32] a model based on the diffusion-reaction rate approach for dry oxidation is reported. In several aspects, the physical picture adopted is not so far from the Deal and Grove model. Molecular oxygen O_2 diffuses in silicon dioxide by a thermally activated process and the hydrostatic pressure influence is neglected.[35] Thus, the reaction between silicon and oxygen is described with this chemical Eq. (13)

$$Si + O_2 \rightarrow SiO_2 \quad (\text{Molecular oxidation}). \tag{13}$$

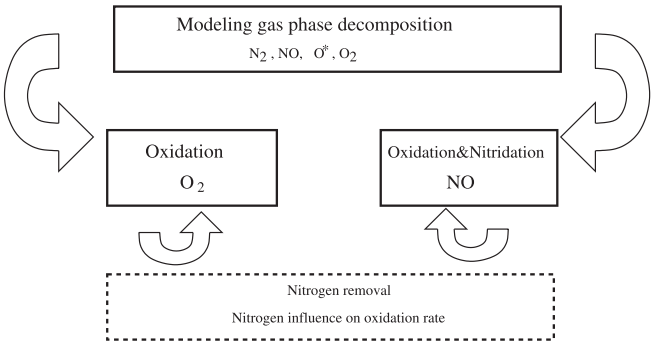

FIG. 7. General strategy proposed in order to simulate the N_2O oxynitridation step. Oxidation O_2 and nitridation and oxidation by NO can be viewed as parallel atomic process.

It could be noticed that in the reaction rate approach framework, the oxidation reaction does not take place strictly at the Si/SiO_2 interface as postulated by the Deal and Grove model.[17] In agreement with some isotopic characterisation,[36] the reaction region is not strictly sharp and can defined in our framework by the overlap between oxygen and silicon concentration. This approach enable probably a better description of the process.

The situation is, however, much more complex than dry oxidation since the presence of nitric oxide (NO) in the gas phase increases the overall complexity. The oxynitridation process could be seen as a parallel oxidation mechanism[37] but with molecular oxygen and nitric oxide. It is assumed here that the nitrous molecule diffuses from the gas phase to the SiO_2. The NO decomposition is supposed to takes place at the silicon interface where a significant Si concentration is present and generates both atomic N^* and O*,

$$NO \rightarrow N^* + O^* \quad (\text{Atomic nitrogen generation}). \tag{14}$$

Theoretically, three different reactions (oxidation, nitridation, and nitrogen removal) have to be considered in the reactive region,

$$\begin{cases} Si + 2O^* & \rightarrow & SiO_2 & (\text{Atomic oxidation}) \\ Si + N^* & \rightarrow & SiN & (\text{Nitridation}) \\ SiN + 2O^* & \rightarrow & SiO_2 + N^* & (\text{Nitrogen removal}). \end{cases} \tag{15}$$

The first one corresponds to the Si oxidation with O*. Two O* atoms are necessary in order to generate SiO_2. Since O* is a very reactive chemical specie,[38] this reaction is probably the most dominant one. The second one is a key mechanism since it corresponds to the Si nitridation and the formation of SiN species in presence of atomic N^*. It has been observed that mostly Si-N bonds are created by nitrous or nitric oxynitridation.[39] Finally, the third one describes the N removal.[40] The presence of O* is known to remove the N incorporated in the silicon and to generate silicon dioxide SiO_2. An intense competition between the last two mechanisms is often put forward to explain the low N^* incorporation into SiO_xN_y (Ref. 40) and the fact that classical oxidation remains the main mechanism in N_2O oxynitridation.

C. The minimal model

A minimal model for N_2O oxynitridation process considering the oxidation by O_2 alone has been set up in the framework of the reaction rate approach. The influence of N is taken into account indirectly. The study of the gas phase decomposition shows that the steady state ambient is mostly composed of O_2 and N_2 (inert). This result can be used in order to build a first order minimal model. As shown in Figure 5, the nitric oxide (NO) molecule in the gas phase has been estimated to be less than 4% in our simulation. All the reactions between the products from NO decomposition and the Si atoms can be neglected in first order to build-up a compact model

$$\begin{cases} \dfrac{\partial n_{[O_2]}}{\partial t} = \nabla(D\nabla n_{[O_2]}) - k_{[N]} n_{[O_2]} n_{[Si]} \\ \dfrac{\partial n_{[Si]}}{\partial t} = -k_{[N]} n_{[O_2]} n_{[Si]} \\ \dfrac{\partial n_{[SiO_2]}}{\partial t} = k_{[N]} n_{[O_2]} n_{[Si]}. \end{cases} \tag{16}$$

This model is close to the previous dry oxidation model related to the reaction rate approach[30,32] except that the reaction rate $k_{[N]}$ governing the reaction between O_2 and Si is dependent on N concentration. Since the nitrogen peak is experimentally strongly localized at the Si/SiO_xN_y interface, a possible influence on O_2 diffusivity has been neglected. The solubility limits of O_2 have also been neglected in this work. It would probably be of interest to refine the model by introducing a limited solubility effect[41] since it impacts the definition of the reaction region. The same Arrhenius law fitted on several dry oxidation experiments in a previous work[32] has been used,

$$D = D_0 \cdot \exp\left(\frac{-E_D}{k_B T}\right), \tag{17}$$

with an activation energy of $E_D = 2.22\,\text{eV}$ and a prefactor $D_0 = 1.291 \times 10^{11}\ \text{nm}^2/\text{s}$.

1. Physical origin of the influence of nitrogen on the oxide growth

The influence of doping on the oxide growth rate has been largely studied in the literature. The mostly accepted physical picture is from the Ho and Plummer[42,43] where the linear growth rate of the Deal and Grove theory is directly related to the concentration of point defects present at the Si/SiO_2 interface. The main defect considered is the Si vacancy since it is linked to the amount of free reaction sites for the oxidation reaction. This theory explains well the fact that a high concentration of doping changes the Fermi level and increases the number of vacancies and thus the oxidation rate. However, it must be stressed that nitrogen is the only species where a reduction of the kinetics is observed.[19,42,44] All the other dopants increase (at various degrees) the reaction rate. Thus, the Ho and Plummer approach cannot be applied to the case where N is incorporated at the interface by oxynitridation or implantation.

The physical origin of the self-limited oxidation mechanism is still not clear. However, some reasonable assumptions can be explained by the kinetics reduction. Nitrogen defects in Si have been studied for many years and it is generally accepted that most of the defects created exist in neutral forms. A possible shift of the Fermi level like in the Ho and Plummer theory has therefore to be excluded. A more direct mechanism has to be considered. The Ab-initio simulations reported in the paper of Goss *et al*. underline the strong interaction between N (mainly nitrogen pairs) and vacancies.[45] The N incorporation at vacancies sites is a plausible explanation to the retardation mechanism since this effect lowers the available free reaction site for the classical oxidation process. A different approach from Ho and Plummer model must be considered in order to take the influence of N into account.

2. Introduction of the influence of nitrogen in the reaction rate expression

Based on the previous analysis, it is assumed that the reaction rate is proportional to the concentration of reactive sites C_{gr},

$$k = k_0 \exp\left(\frac{-E_A}{k_b T}\right) C_{gr}. \tag{18}$$

The free reacting sites concentration (C_{gr}) is thus directly related to the nitrogen species SiN. From Sec. III B describing the interaction between atomic nitrogen and silicon, it can be deduced that the presence of SiN specie is governed by the competition between nitridation[46] and nitrogen removal[40]

$$\frac{\partial n_{[SiN]}}{\partial t} = k_{[N^*]} n_{[N^*]} n_{[Si]} - k_{removal} n_{[O^*]} n_{[SiN]}. \tag{19}$$

C_{gr} follows an equivalent equation with generation and recombination terms. The recombination can be attributed to the nitridation reaction which removes growing sites while the generation part is associated to the nitrogen removal reaction and the generation of defects during the oxidation process[47]

$$\frac{\partial C_{gr}}{\partial t} = G - R. \tag{20}$$

Assuming that the generation term has the same activation energy as the reaction rate of a dry oxidation, leads to Eq. (21),

$$G = G_0 \exp\left(\frac{-E_A}{K_B T}\right), \tag{21}$$

and the recombination terms to be proportional to the concentration of growth sites C_{gr},

$$R = \frac{C_{gr}}{\tau}. \tag{22}$$

At the beginning of the oxynitridation process, since no SiN species are present, the following expression is obtained:

$$C_{gr} = a_0 \exp\left(\frac{-E_{A'}}{k_b T}\right) + b_0 \exp\left(\frac{-t}{\tau}\right) \exp\left(\frac{-E_{A'}}{k_b T}\right), \tag{23}$$

where a_0, b_0, $E_{A'}$, and τ are new parameters. This equation leads to the final expression Eq. (24) for reaction k in the case of N_2O

$$k = a_0 \exp\left(\frac{-E_{A'}}{k_b T}\right)\left[1 + b_0 \exp\left(\frac{-t}{\tau}\right)\right]. \tag{24}$$

D. Calibration

The compact model needs the following four parameters: $E_{A'}$, a_0, b_0, and τ. The parameters were adjusted on the oxidation kinetics of Ting *et al*.[13] reported in Sec. IV A. Several numerical procedures have been tested (least square methods, simulated annealing) in order to determine the best parameters set. Most of the fits lead to unphysical parameters and, to reach a physical solution in the initial regime, the value of the reaction rate k should be close to that used for dry oxidation.[32] Reasonable physical parameters were reported in the next Table III in order to describe the reaction rate in presence of N. The characteristic time τ which can be viewed as the time step necessary to incorporate a sufficient amount of N. It was obtained by the calibration step for a given temperature range. An Arrhenius law given by the next Eq. (25) was observed

$$\frac{1}{\tau} = 86.96 \exp\left(\frac{-1}{k_b T}\right). \tag{25}$$

With the help of Eq. (25) and the parameters given in Table III, the reaction rate given in Eq. (24) was calculated in the temperature range considered (Fig. 8). The mathematical system is made of three coupled Eqs. (16). This system is numerically solved using a Crank-Nicolson method.[28]

IV. COMPARISON BETWEEN THE COMPACT MODEL AND EXPERIMENTAL RESULTS

It is difficult to assess the physical validity of an oxidation model by simply considering the quality of the agreement between the theoretical oxidation kinetics and some experimental data as previously elegantly underlined by Blanc.[48] A particular attention on the physical relevance of the kinetics parameters should be paid too.[49] On the other hand, it is often needed to evaluate the practical capability and the limits of a oxidation model in order to describe the experimental oxidation kinetics specially in the ultra-thin

TABLE III. Parameters for the reaction rate expression of the compact model.

$E_{A'}$	1.42 eV
a_0	10^{+06} nm/s^{-1}
b_0	11

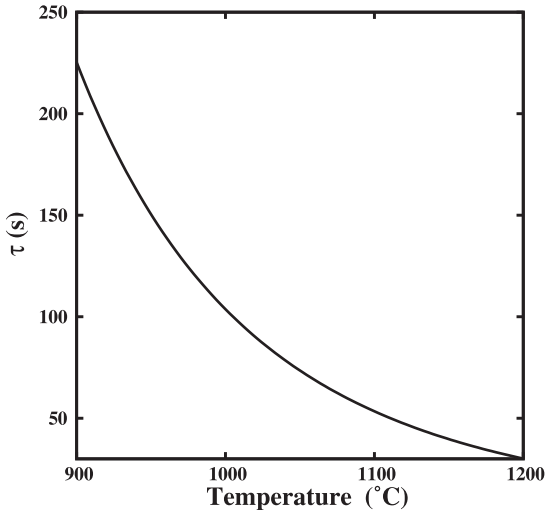

FIG. 8. Variation of the characteristic time τ with the furnace temperature. τ varies from 40 s at 1150 °C up to 225 s at 800 °C. The values are compatible with the time necessary to incorporate a sufficient amount of nitrogen to strongly reduce the oxidation kinetics.

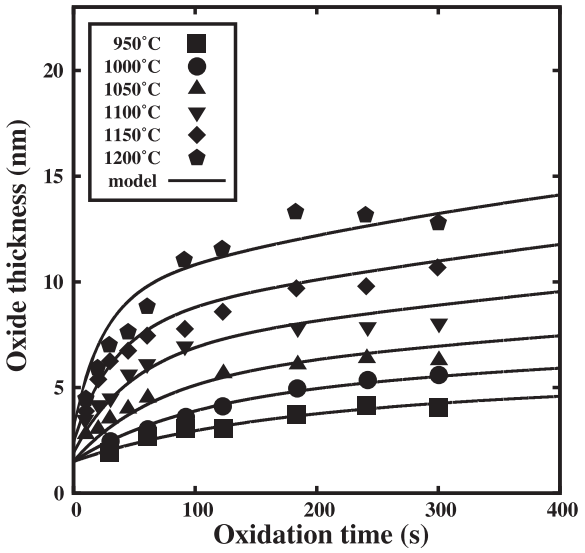

FIG. 9. Comparison between the minimal model and the kinetics of Ting *et al*. The oxidation kinetics is clearly limited by the nitrogen incorporation after a time around 50 s.

regime. The compact model was compared to several experimental kinetics available in the literature. A particular attention was paid to the kind of furnace (rapid thermal annealing or classical). It was claimed experimentally that the nitrogen incorporation or the N profile is highly dependent on gas process parameters such as input flow rate[29] or on the type of furnace used.[50]

A. Test with rapid thermal annealing experiments

The minimal model was compared to the experiments of Ting *et al*.[13] The experiments were performed with a commercial lamp-heated rapid thermal processor. The oxidation temperature ranged from 950 °C to 1200 °C with increments of 50 °C and oxidation times from 10 to 300 s. It has been estimated that the average concentration in the grown oxide are less than 4% at the interface. The experimental kinetics is first characterized by a short fast initial regime and next followed by a strongly limited oxidation range. To facilitate the comparison between the model and these experiments, the simulated kinetics was shifted vertically in order to match the experimental oxide thickness at the end of the temperature ramp-up. The shift is between 1.5 nm for the lowest temperature up to 2.4 nm for 1150 °C. The comparison between the model and these experiments are in excellent agreement from the previous calibration. As shown in the Figure 9, the fast initial time for high temperature is well described. A nice agreement is obtained in the self-limited oxidation regime where oxidation is strongly reduced by the nitrogen incorporation. Left alone, the initial oxide thickness concern, the trends and the variations of oxide growth are well described. Next, the comparison with the experimental kinetics from Yoon *et al*.[51] was undertaken (Fig. 10). The growth of ultra-thin (3–10 nm) oxynitride films was performed using a specific designed furnace (vertical gas flow and rotation of the substrate). The authors report an excellent uniformity for the oxides grown (5%) since the N_2O oxidation is more sensitive to the process variation. The oxidation times are much shorter here between [20–100] s and the self-limited regime is then less visible. The agreement with the model remains very good if it is assumed that the initial temperature ramp-up creates an initial oxynitride of about 2.5 nm.

B. Test with classical furnace experiments

Next, the model has been compared to the experimental work of Soleimani *et al*.[52] These oxynitridation experiments were undertaken in an ambient of pure N_2O at a pressure of 500 Torr and three relatively low temperatures (885 °C, 935 °C, and 975 °C). Much larger oxidation times are required here from 20 min up to 120 min in order to grow a significant oxide thickness (Fig. 11). Only the experimental

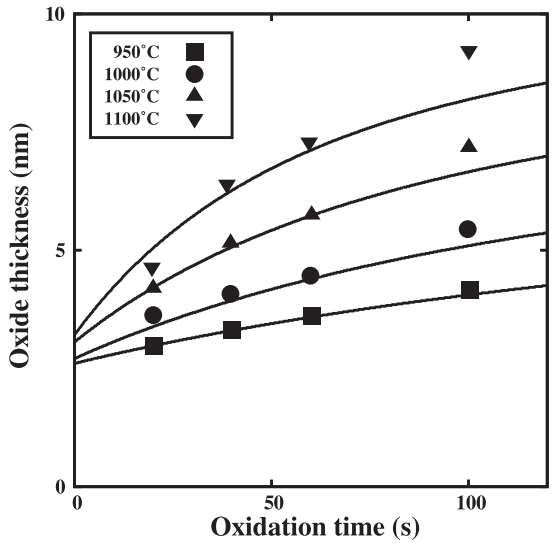

FIG. 10. Comparison between the minimal model and the kinetics of Yoon *et al*.[51]

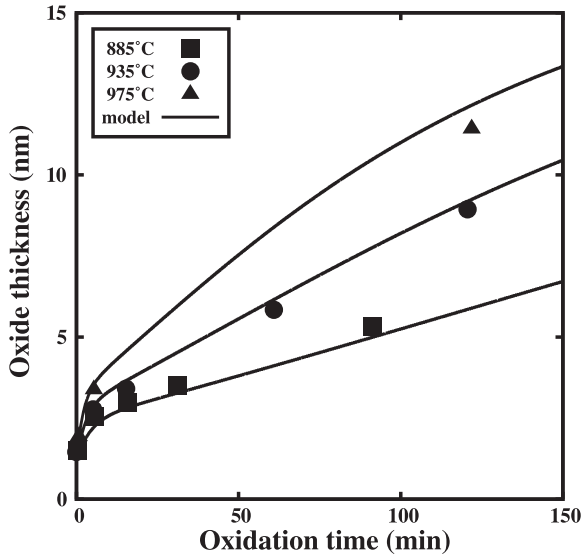

FIG. 11. Comparison between the minimal model and the kinetics of Philipossian *et al*.

kinetics with the lowest initial oxide thickness (1.5 nm) was considered.[53] An overall good agreement is observed between the theory and experiments. The main discrepancy is observed for the last point at 935 °C but the error remains lower than 1 nm for the other points. Finally, the experiments of Bhat *et al*.[54] have also been studied (Fig. 12). Here, the oxidation experiments were performed in a classical temperature heated furnace. A dry ambient, during the temperature ramp-up, has been used to prevent an initial surface nitridation. The experiments are very similar to those of Soleimani *et al*. with large oxidation times and a temperature around 1000 °C. Again an overall good agreement is obtained and the trends are in agreement with the experiments. The only exception is for the highest temperature where the model predicts a more self-limited oxidation regime. However, it should be kept in mind that the N diffusion/out-diffusion could not be neglected for these long oxidation times.

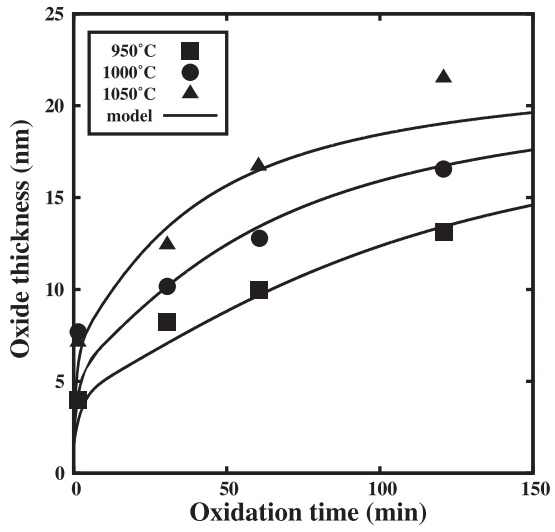

FIG. 12. Comparison between the minimal model and the kinetics of Bhat *et al*.[54]

V. CONCLUSION

Some progress in the modelling of N_2O oxynitridation process is reported. The steady state concentration of O_2 and NO was estimated through the modelling of the gas phase decomposition. A general model based on the reaction rate approach which described the large competition between nitridation and nitrogen removal was specified. A minimal model where only the oxidation with O_2 is simulated was implemented and calibrated. The influence of molecular nitrogen in the reaction rate has been successfully incorporated. Although the minimal model was adjusted on rapid thermal annealing experiments, it has been able to give a correct trend both in the thin and the limited regime observed for a longer oxidation. The kinetics predicted by the model is in good agreement with several experimental works. Current limits and a possible strategy to access to a complete modelisation of the NO, N_2O oxynitridation processes and to the N profile have been discussed.

ACKNOWLEDGMENTS

The author thanks Wilfried Lerch for suggesting the industrial interest of N_2O oxynitridation. This work was supported by the European Commission with the former European Project FRENDTECH (IST-2000-30129).

[1]See http://www.eetimes.com/news/semi/showArticle.jhtml?articleID=210604347 for "Tsmc pushes out high-k in 28-nm rollout."
[2]H. Chung, J. Niess, W. Dietl, G. Roters, W. Lerch, Z. Nenyei, A. Ludsteck, J. Schulze, I. Eisele, K. Wieczorek *et al*., Semicond. Int. **27**, 73 (2004).
[3]H. Fukuda, M. Yasuda, T. Iwabucchi, and S. Ohno, IEEE Electron Device Lett. **12**, 587 (1991).
[4]A. B. Joshi, G. Yoon, G. Q. Lo, and D.-L. Kwong, IEEE Trans. Electron Devices **40**, 1437 (1993).
[5]H. Hwang, W. Ting, D. L. Kwong, and J. Lee, IEEE Electron Device Lett. **12**, 495 (1991).
[6]A. Philipossian and D. B. Jackson, J. Electrochem. Soc. **139**, L82–L83 (1992).
[7]T. Hori, H. Iwasaki, T. Ohmura, and Y. Yoshioka, J. Appl. Phys. **65**, 629 (1989).
[8]Y. Okada, P. J. Tobin, K. G. Reid, R. I. Hegde, B. Maiti, and S. A. Ajuria, IEEE Trans. Electron Devices **41**, 1608 (1994).
[9]R. I. Hegde, P. J. Tobin, K. G. Reid, B. Maiti, and S. Ajuria, Appl. Phys. Lett. **66**, 2882 (1995).
[10]M. Bhat, L. K. Han, D. Wristers, J. Yan, D. L. Kwong, and J. Fulford, Appl. Phys. Lett. **66**, 1225 (1995).
[11]Z.-Q. Yao, H. B. Harrisson, S. Dimitrijev, and Y. T. Yeow, IEEE Electron Device Lett. **15**, 516 (1994).
[12]H. Hwang, W. Ting, B. Maiti, D.-L. Kwong, and J. Lee, Appl. Phys. Lett. **57**, 1010 (1990).
[13]W. Ting, H. Hwang, J. Lee, and D. L. Kwong, J. Appl. Phys. **70**, 1072 (1991).
[14]G. Q. Lo, W. Ting, J. Ahn, and D. L. Kwong, IEEE Electron Device Lett. **13**, 111 (1992).
[15]J. Ahn, W. Ting, and D. L. Kwong, IEEE Electron Device Lett. **13**, 117 (1992).
[16]A. Bauer and E. Burte, Microelectron. J. **27**, 667 (1996).
[17]B. E. Deal and A. S. Grove, J. Appl. Phys. **36**, 3770 (1965).
[18]S. Dimitrijev, H. B. Harrison, and D. Sweatman, IEEE Trans. Electron Devices **43**, 267 (1996).
[19]H. R. Soleimani, B. S. Doyle, and A. Philipossian, J. Electrochem. Soc. **142**, L132 (1995).
[20]A. Morales-Acevedo, G. Santana, and J. Carillo-Lopez, Journal of The Electrochemical Society **148**, F200 (2001).

[21]E. C. Carr, K. A. Ellis, and R. A. Buhrman, Appl. Phys. Lett. **66**, 1492 (1995).
[22]C. S. Mian and L. S.-Y. Flora, Solid-State Electron. **43**, 1997 (1999).
[23]E. P. Gusev, H. C. Lu, E. Garfunkel, T. Gustafsson, M. L. Green, D. Brasen, and W. N. Lennard, J. Appl. Phys. **84**, 2980 (1998).
[24]S. S. Dang and C. G. Takoudis, J. Appl. Phys. **86**, 1326 (1999).
[25]M. J. Hartig and P. J. Tobin, J. Electrochem. Soc. **143**, 1753 (1996).
[26]A. Gupta, S. Toby, E. P. Gusev, H. C. Lu, Y. Li, M. L. Green, T. Gustafsson, and E. Garfunkel, Prog. Surf. Sci. **59**, 103 (1998).
[27]K. A. Ellis and R. A. Buhrman, IBM J. Res. Dev. **43**, 287 (1999).
[28]W. Press, S. A. Teukolsky, W. T. Vetterling, and B. P. Flannery, *Numerical Recipes in Fortran 77: The Art of Scientific Computing* (Cambridge University Press, 1986).
[29]P. J. Tobin, Y. Okada, S. A. Ajuria, V. Lakhotia, W. A. Feil, and R. I. Hedge, J. Appl. Phys. **75**, 1811 (1994).
[30]R. M. C. de Almeida and I. J. R. Baumvol, Phys. Rev. B **62**, R16255 (2000).
[31]R. M. C. de Almeida, I. J. R. Baumvol, J. J. Ganem, I. Trimaille, and S. Rigo, J. Appl. Phys. **95**, 1770 (2004).
[32]C. Krzeminski, G. Larrieu, J. Penaud, E. Lampin, and E. Dubois, J. Appl. Phys. **101**, 064908 (2007).
[33]In case of an incomplete decomposition, atomic oxygen for example O* should be introduced.
[34]It corresponds to the different silicon-nitrogen species.
[35]This assumption cannot be done for nano-object oxidation.
[36]F. Rochet, B. Agius, and S. Rigo, J. Electrochem. Soc. **131**, 914 (1984).
[37]C.-J. Han and C. R. Helms, J. Electrochem. Soc. **134**, 1297 (1987).
[38]Y. Ishikawa, Y. Takagi, and I. Nakamichi, Jpn. J. Appl. Phys., Part 2 **28**, L1453 (1989).
[39]Z. Yao, J. Appl. Phys. **78**, 2906 (1995).
[40]N. S. Saks, D. I. Ma, and W. B. Fowler, Appl. Phys. Lett. **67**, 374 (1995).
[41]E. Antoncik, Appl. Phys. A **58**, 117 (1994).
[42]C. P. Ho and J. D. Plummer, J. Electrochem. Soc. **126**, 1516 (1979).
[43]C. P. Ho and J. D. Plummer, J. Electrochem. Soc. **126**, 1523 (1979).
[44]C. R. Fritzsche and W. Rothemund, J. Electrochem. Soc. **120**, 1603 (1973).
[45]J. P. Goss, I. Hahn, R. Jones, P. R. Briddon, and S. Oberg, Phys. Rev. B **67**, 045206 (2003).
[46]V. A. Gritsenko, H. Wong, W. M. Kwok, and J. B. Xu, J. Vac. Sci. Technol. B **21**, 241 (2003).
[47]D. Skarlatos, D. Tsoukalas, L. F. Gilles, and A. Claverie, J. Appl. Phys. **87**, 1103 (2000).
[48]J. Blanc, Philos. Mag. B **55**, 685 (1987).
[49]P. Roura and J. Farjas, Phys. Rev. B **74**, 127301 (2006).
[50]E. C. Carr and R. A. Buhrman, Appl. Phys. Lett. **63**, 54 (1993).
[51]G. W. Yoon, A. B. Joshi, J. Ahn, and D. L. Kwong, J. Appl. Phys. **72**, 5706 (1992).
[52]H. R. Soleimani, A. Philipossian, and B. Doyle, Tech. Dig.-Int. Electron Devices Meet. **1992**, 631.
[53]Various initial oxide thickness grown in dry conditions have been considered in the study of Soleimani *et al*. and only a vertical shift of the various N_2O kinetics has been observed.
[54]M. Bhat, H. Jia, and D. L. Kwong, J. Appl. Phys. **78**, 2767 (1995).